

Polymer Chemistry

Accepted Manuscript



This is an *Accepted Manuscript*, which has been through the Royal Society of Chemistry peer review process and has been accepted for publication.

Accepted Manuscripts are published online shortly after acceptance, before technical editing, formatting and proof reading. Using this free service, authors can make their results available to the community, in citable form, before we publish the edited article. We will replace this *Accepted Manuscript* with the edited and formatted *Advance Article* as soon as it is available.

You can find more information about *Accepted Manuscripts* in the [Information for Authors](#).

Please note that technical editing may introduce minor changes to the text and/or graphics, which may alter content. The journal's standard [Terms & Conditions](#) and the [Ethical guidelines](#) still apply. In no event shall the Royal Society of Chemistry be held responsible for any errors or omissions in this *Accepted Manuscript* or any consequences arising from the use of any information it contains.



Journal Name

ARTICLE

Polyamide 6/silica hybrid materials by a coupled polymerization reaction

L. Kaßner^a, K. Nagel^a, R.-E. Grützner^b, M. Korb^c, T. Rüffer^c, H. Lang^c and S. Spange^a

Received 00th January 20xx,
Accepted 00th January 20xx

DOI: 10.1039/x0xx00000x

www.rsc.org/

Polyamide 6/SiO₂ hybrid materials were produced by a coupled polymerization reaction of three monomeric components namely 1,1',1'',1'''-silanetetrayltetrakis-(azepan-2-one) (Si(ε-CL)₄), 6-aminocaproic acid (ε-ACA) and ε-caprolactam (ε-CL) within one process. Si(ε-CL)₄ together with ε-ACA has been found suitable as precursor monomer for the silica and PA6 component. The accurate adjusting of the molar ratio of both components, as well as the combination of the overall process for producing the polyamide 6/SiO₂ hybrid material with the hydrolytic ring opening polymerization of ε-caprolactam is of great importance to achieve homogeneous products with a low extractable content. Water in comparison to ε-ACA has been found unsuitable as oxygen source to produce uniformly distributed silica. The procedure was carried out in a commercial laboratory autoclave at 8 bar initial pressure. The molecular structure and morphology of the hybrid materials have been investigated by solid state ²⁹Si and ¹³C NMR spectroscopy, DSC, FTIR spectroscopy and electron microscopic measurements.

Introduction

Polyamide 6 (PA6) is one of the most important engineering plastics, due to the combination of high mechanical and thermal stability, chemical resistance and processability.¹ Physical properties can be further improved by combination with other components, e.g. layered silicates^{2–4}, glass or carbon fibres^{5–8} and metal oxides,^{9–12} to fabricate hybrid materials or composites. These materials are suitable for several applications, especially in automobile industry, for example as inlet for fuel systems, wheel trims and engine covers.¹³ PA6/silica hybrid materials are of special interest because incorporation of SiO₂ into PA6 improves mechanical properties such as hardness and elastic modulus.^{14,15} Furthermore, silica is non-toxic, colorless and nanoparticles as well as hybrid materials could be obtained by the sol-gel process at mild reaction conditions.

Strategies for producing PA6/SiO₂ hybrid materials can be classified in different categories. In the simplest way, both components, the preformed SiO₂ and PA6, are mixed together by extrusion, melting or another appropriate procedure.^{16–21} More elegant ways use the *in situ* formation of the SiO₂ component, i.e. by sol-gel processing²² or the *in situ* polymerization of ε-caprolactam in presence of preformed silica particles.^{15,23–26} The grafting of PA6 on surface functionalized SiO₂ particles is also a suitable route to fabricate

polymer/SiO₂ hybrid materials.^{27,28} As an additional way, the simultaneous formation of both polymer components within one procedure is known.^{14,29} So far, there is no report on the simultaneous synthesis of PA6 and SiO₂ from a combined monomer within one coupled polymerization reaction.

In the literature the terms composite and hybrid material have been used in different ways for those types of materials.¹⁶ Composite materials are mixtures of both components on a length scale of 100 nm to 10 m, whereas inorganic/organic hybrid materials are combined at the molecular level up to several nm. The challenge is to create nanostructured hybrid materials, which show a stronger improvement in physical properties than macroscopic mixtures even at low filler contents of a few weight percent.

To achieve a nanostructured hybrid material, the simultaneous formation of both components in vicinity is required.³⁰ Therefore, monomers have been constructed in such a way that two polymers are formed from one single source monomer. This strategy has been established for monomers which contain two different moieties suitable for polymerization, one for chain polymerization and another one, i.e. for sol gel processes.^{31–34} However, in this case both groups do polymerize independently of each other. For step-growth polymerization processes, the twin polymerization has been established as an elegant route to fabricate nanostructured inorganic/organic hybrid materials. The formation of both polymers occurs mechanistically coupled, which is the reason for the smooth nanostructure formation.^{30,35,36} Monomers which are used in twin polymerization are called twin monomers.

The objective of this publication is the development of a coupled polymerization procedure for synthesis of PA6/SiO₂

^a Polymer Chemistry, Technische Universität Chemnitz, 09107 Chemnitz, Germany.

^b BASF SE, Carl-Bosch-Str. 38, 67063 Ludwigshafen am Rhein, Germany.

^c Inorganic Chemistry, Technische Universität Chemnitz, 09107 Chemnitz, Germany; pertaining single X-ray structure analysis.

^d † Electronic Supplementary Information (ESI) available. See DOI: 10.1039/x0xx00000x

hybrid materials within one process. Therefore, three different reactants, namely 1,1',1'',1'''-silanetetrayltetrakis-(azepan-2-one) ($\text{Si}(\epsilon\text{-CL})_4$), 6-aminocaproic acid ($\epsilon\text{-ACA}$) and $\epsilon\text{-caprolactam}$ ($\epsilon\text{-CL}$) are used in different ratios to adjust the amount of formed silica. The combined monomer $\text{Si}(\epsilon\text{-CL})_4$ **1** which contains the $\epsilon\text{-caprolactam}$ moiety covalently bound via the *N*-atom to the silicon is used as precursor for the formation of silica as well as polyamide 6. Basically for the purpose of PA6 production cyclohexanone oxime (CHO) as industrial precursor molecule for $\epsilon\text{-CL}$ seems also eligible as component in monomer **2** $\text{Si}(\text{CHO})_4$ (Scheme 1). However, in this case the BECKMAN rearrangement of this monomer would be an essential step before polymerization takes place.

Both types of silicon monomers are investigated for PA6/SiO₂ hybrid material synthesis. It must be mentioned, that the single polymerization of **1** or **2** is unsuitable to produce PA6/SiO₂ as the overall stoichiometry is not complied. Water is essential as co-component (Scheme 2). Therefore it must be emphasized that monomer **1** and **2** are not ideal twin monomers but they are related to deficient twin monomers due to the possible mechanistically coupled formation of the inorganic and organic polymer. The polymerization process as shown in Scheme 2 is related to the apparent twin polymerization.³⁷

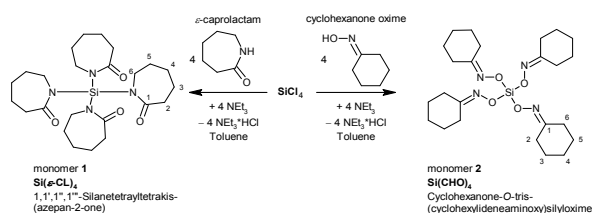
The challenge of PA6/SiO₂ hybrid material synthesis according to Scheme 2 is the improvement of the operative coupling of several reactions. One crucial aspect is how the water equivalent can be realized among the occurring processes. Water can be used directly or from a suitable source like the polycondensation of 6-aminocaproic acid. $\epsilon\text{-ACA}$ seems to be eligible, because it polymerizes to PA6 and initiates the hydrolytic lactam polymerization. The coupling of the water delivering and the water consuming reaction (equation 1 and 2 in Scheme 2) to produce PA6/SiO₂ has been explored as function of the ratio of **1** and $\epsilon\text{-ACA}$. As a third reaction component $\epsilon\text{-caprolactam}$ has been found suitable for a good homogenization of the reaction melt (according to equation 3 in Scheme 2). By variation of reactant concentrations different SiO₂ amounts are adjustable. The reactions have been carried out in a typical procedure, which is suitable to fabricate PA6 from $\epsilon\text{-CL}$.

Experimental

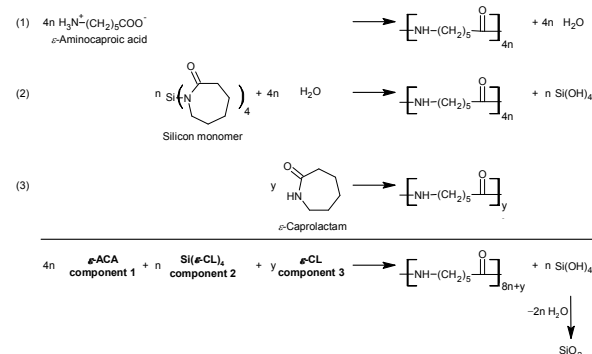
Materials and methods

$\epsilon\text{-Caprolactam}$ (> 99%) and silicon tetrachloride (99%) were purchased from Sigma Aldrich. 6-Aminocaproic acid (99%) was purchased from Alfa Aesar. Cyclohexanone oxime (97 %) was ordered from Acros. Toluene was dried by standard methods and distilled before use in argon atmosphere. CDCl_3 was dried with molecular sieve 4 Å and stored under argon.

Liquid state ¹H NMR (250.1 MHz), ¹³C NMR (62.9 MHz) and ²⁹Si NMR (49.7 MHz) spectra were measured with a Bruker Avance 250 NMR spectrometer. The residual signal of the solvent CDCl_3 was used as internal standard ($\delta = 7.26$ ppm).



Scheme 1 Molecular structures of silicon monomers derived from $\epsilon\text{-caprolactam}$ (monomer **1**) and cyclohexanone oxime (monomer **2**). For synthetic procedure see Experimental Part.



Scheme 2 Strategy for fabrication of PA6/SiO₂ hybrid materials by coupling the reaction of $\text{Si}(\epsilon\text{-CL})_4$ with the polycondensation of $\epsilon\text{-ACA}$ among the hydrolytic ring opening polymerization of $\epsilon\text{-CL}$.

Solid state NMR spectra were recorded using a Bruker Digital Avance 400 spectrometer, equipped with double tuned probes capable of MAS (magic angle spinning). ¹³C{¹H}-CP-MAS NMR spectra were measured at 100.6 MHz using 3.2 mm standard zirconium oxid rotors spinning at 15 kHz. ²⁹Si{¹H}-CP-MAS NMR spectra were recorded at 79.5 MHz with a sample spin rate of 12 kHz. Cross polarization with a contact time of 3 ms was used to enhance sensitivity. The recycle delay was 6 s. The spectra were referenced externally to tetramethylsilane (TMS) (¹H, $\delta = 0$ ppm) and adamantane (¹³C, $\delta = 38.5$ ppm). The spectra were collected with ¹H decoupling using TPPM pulse sequence.

DSC measurements were performed by a DSC 1 (Mettler Toledo). All measurements were done in 40 μL aluminium pans and a N_2 -flow of 50 $\text{mL}\cdot\text{min}^{-1}$ in a temperature range from 25–250 °C with a heating rate of 10 $\text{K}\cdot\text{min}^{-1}$. In cyclic measurements with two heating segments and one cooling segment, the highest, respectively lowest temperature was held for 2 min.

ATR-FTIR spectra were obtained with a Golden Gate ATR accessory from LOT-Oriel GmbH & Co. KG, Darmstadt, using a BioRad FT-IR 165 spectrometer (Bio-Rad Laboratories, Philadelphia, PA, USA).

The molecular weight distribution of PA6 was determined by SEC at BASF SE using an App_P apparatus with SDV as stationary phase, the column temperature was 65 °C. 1,1,1,3,3,3-Hexafluoro-2-propanol containing 0.05 % of potassium trifluoroacetate was used as eluent with an elution rate of 1 $\text{mL}\cdot\text{min}^{-1}$ and the sample concentration was

1.5 mg·mL⁻¹. PMMAs of narrow and defined molecular weights were used as calibration standards.

The transmission electron microscopy (TEM) was carried out using the Libra 120 (120 kV) transmission electron microscope of Zeiss by TEM Laboratory, BASF SE. Before the measurements, ultra thin cuts were performed by a Leica ultramicrotome EM UC7 and cryogenic chamber Leica EM FC7 (80–120 nm).

Electron microscopic images were taken by an instrument from type Nova NanoSEM 200 of FEI Company after sputtering with platinum (TU Chemnitz, Laboratory of Solid Surfaces Analysis).

Single crystal X-ray structural analyses were performed with an Oxford Gemini diffractometer with Cu-K α -radiation (λ = 154.184 pm) at TU Chemnitz, Laboratories of Inorganic Chemistry.

Quantitative elemental analysis of the elements C, H and N were done with varioMICRO CHNS from Elementar Analysensysteme GmbH (TU Chemnitz, Laboratory of Organic Chemistry).

Thermogravimetric measurements were realized on a Thermogravimetric Analyzer 7 (TGA 7), of Perkin Elmer Company (TU Chemnitz, Laboratory of Physical Chemistry). First the samples were heated from 30–700 °C with a heating rate of 20 K·min⁻¹ under constant Helium flow. Under further heating to 900 °C the gas flow switched to air. This temperature was held for another 30 min.

Synthesis of monomer 1 and 2

In a typical procedure, either ϵ -caprolactam or cyclohexanone oxime (20.0 g, 0.177 mol) was dissolved under stirring in anhydrous toluene (300 mL). Triethylamine (20.2 g, 0.200 mol) was added in slight excess in a single portion. This solution was cooled by water bath and SiCl₄ (7.5 g, 0.044 mol), dissolved in 100 mL anhydrous toluene, was added slowly through a dropping funnel under vigorous stirring. Immediately a white precipitate from triethylammonium chloride was observed. Subsequently, the solution was stirred at room temperature for 16 h. Triethylammonium chloride was separated by filtration. After removing of the solvent under vacuum, a white to beige solid was obtained.

1,1',1'',1'''-Silanetetrayltetrakis(azepan-2-one) **1**:

yield: 80 %. δ_{H} /ppm (250 MHz; CDCl₃): 1.62–1.72 (24 H, m, 3-H–5-H), 2.44–2.45 (8 H, m, 1-H), 3.19 (8 H, m, 6-H). δ_{C} /ppm (63 MHz; CDCl₃): 23.6, 29.6, 30.3 (C-3–C-5), 38.3 (C-2), 46.1 (C-6), 183.9 (C-1). δ_{Si} /ppm (50 MHz; CDCl₃): –43.5. ν_{max} /cm⁻¹: 2915, 2857 (CH₂), 1638 (C=O), 922 (Si–N). Found: C, 60.17; H, 9.23; N, 11.64. Calc. C₂₄H₄₀N₄O₄Si: C, 60.47; H, 8.46; N, 11.75.

Cyclohexanone-O-tris(cyclohexylideneaminoxysilyloxime) **2**:

yield: 82 %. δ_{H} /ppm (250 MHz; CDCl₃): 1.61 (24 H, m, 3-H–5-H), 2.25 (8 H, t, ³J₅₆ = 8.0 Hz, 6-H), 2.60 (8 H, t, ³J₂₃ = 8.0 Hz, 2-H). δ_{C} /ppm (63 MHz; CDCl₃): 27.1, 25.9, 25.7 (C-2–C-5), 32.2 (C-6), 167.1 (C-1). δ_{Si} /ppm (50 MHz; CDCl₃): –73.7. ν_{max} /cm⁻¹: 2931–2857 (CH₂), 1638 (C=N), 1447 (CH₂), 940 (Si–O). Found: C, 59.51; H, 8.49; N, 11.53. Calc. C₂₄H₄₀N₄O₄Si: C, 60.47; H, 8.46; N, 11.75.

Table 1 Summary of obtained samples with molar ratios of reactants used and amount of extractables. The sample name gives information about SiO₂ amount. For example, **P1** stands for a hybrid material with 1 wt% of SiO₂. Furthermore the endorsement **P1_x** means that a variation of molar ratios of reactants for the special SiO₂ content was chosen.

No.	SiO ₂ amount	Molar ratios of reactants			Extractables (48 h, MeOH)
		ϵ -ACA	Si(ϵ -CL) ₄ 1	ϵ -CL	
R	Reference (pure PA6)	1	0	4.4	10.0 %
P1_1	1 wt% SiO ₂	10	1	38.6	13.9 %
P1_2	1 wt% SiO ₂	7.2	1	41.4	18.7 %
P1_3	1 wt% SiO ₂	4	1	43.5	31.9 %
P2	2 wt% SiO ₂	4.3	1	18	13.9 %
P5_1	5 wt% SiO ₂	4	1	1.2	11.5 %
P5_2	5 wt% SiO ₂	2.4	1	3.7	21.0 %

Synthesis of hybrid materials

Composites were synthesized with a high pressure lab autoclave of Berghof company. A Teflon beaker was used as insert. Before heating to reaction temperature of 230 °C, the reactants ϵ -ACA, ϵ -CL and **1** were filled in the autoclave in the specified molar ratios (Table 1) at room temperature and then it was purged with Argon up to 8 bar and afterwards relaxed to atmospheric pressure thrice. The reaction took place under 8 bar initial pressure (argon) for at least 210 min, including ca. 60 min heating phase. During reaction, pressure increased to approximately 14 bar. 15 min before termination of reaction time, pressure was released slowly to start post condensation phase. After cooling down to ambient temperature, the white to beige-colored monolithic samples were crushed into smaller pieces. To remove residual monomers or oligomers the hybrid materials were purified by soxhlet extraction for 48 h with methanol and then dried in a vacuum oven at 40 °C to constant mass. The reference was synthesized according to the same polymerization procedure except the addition of **1**. To increase average molecular weight a post condensation reaction can be carried out at 200 °C and 5 mbar for 12 h afterwards.

The hybrid material synthesis procedure is reproducible for several times. For further information of the reproducibility by the example of **P2** see ESI[†] (Fig. S1 for ATR-FTIR spectra, Fig. S2 for DSC traces and Table S1 for amount of extractables and quantitative elemental analysis).

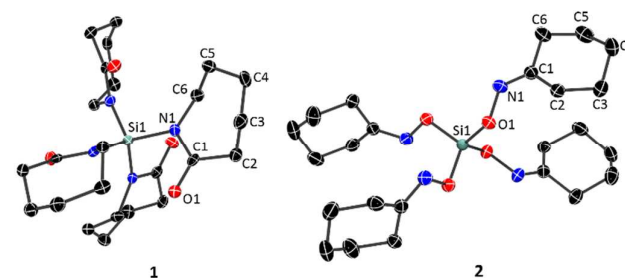


Fig. 1 ORTEP drawing of monomers **1** (left) and **2** (right), with ellipsoids drawn at the 50% probability level. Hydrogens are omitted for clarity.

Results and Discussion

Both monomers **1** and **2** were not described accurately in the literature. **1** is only briefly mentioned in a patent.

The synthesis for **1** and **2** has been done by reaction of SiCl_4 with $\epsilon\text{-CL}$ or cyclohexanone oxime using an appropriate amine base to bind the HCl (see Experimental Part). Both new monomers have been characterized by spectroscopic methods and single X-ray structure analysis. Figure 1 shows the molecular structures of the synthesized monomers. For bond lengths and angles, as well as data acquisition details see ESI† (Table S2, S3 and S4). Both molecules have a S_4 -symmetry with tetrahedral geometry at the silicon atom. Bonding to silicon causes planarization of the nitrogen atoms (sum of angles at the nitrogen atoms $\sim 359^\circ$).^{38–41} Conspicuous in **1** is the small distance of 2.77 Å between Silicon and Oxygen in the solid state, which is shorter than the sum of the van der Waals radii of the Si and O atom (3.62 Å).⁴² Comparable Si–O and Si–N distances were found by RONG and WOLLENWEBER *et al.* who discussed comparable structures with tosyl groups as substituents at the nitrogen atoms in terms of a [4+4] octacoordination with a tetrahedral SiN_4 core and four oxygen atoms in the “outer sphere”, capping the tetrahedral planes.^{43–45} The chemical shift of the ^{29}Si NMR signals of monomer **1** in solid state and solution state are similar which indicates the same bonding motif (Fig. S3 in ESI†). The solid state ^{29}Si NMR signal appears at $\delta = -43.0$ ppm, which could be explained by the electron withdrawing effect of the carbonyl groups next to the nitrogen atom. Therefore, no strong effect of an octacoordination could be observed by ^{29}Si NMR spectroscopy. Consequently, it is unclear whether the short Si–O distances are due to an additional stabilization or just steric reasons. All attempts to polymerize **2** to any PA6 hybrid materials failed. It remains intractable for BECKMANN rearrangement towards the $\epsilon\text{-CL}$ component. Neither acid treatment nor heating in different melt compositions have been successful (Table S5 in ESI†). Therefore, solely **1** was further investigated for hybrid material synthesis.

In spite of the fact that water is suitable to induce the thermal polymerization of $\epsilon\text{-CL}$, the use of free water as source for the synthetic procedure was not favorable because of a lower conversion or discoloration of the products (Table S6 in ESI†). The amino acid $\epsilon\text{-ACA}$ as water source has been found to be the most convenient way.

In preliminary studies, the reaction of **1** with $\epsilon\text{-ACA}$ has been studied by DSC measurements to optimize the polymerization temperature for the overall process (Fig. 2). Monomer **1** shows a complex temperature dependence. However melting and polymerization of $\epsilon\text{-ACA}$ at temperatures $\geq 209^\circ\text{C}$ is in sum endotherm due to the evaporation of the arising water. The combination of $\epsilon\text{-ACA}$ with **1** leads to a decrease of the polymerization temperature below 200°C . In addition, an increasing $\epsilon\text{-ACA}$ amount requires a higher reaction temperature. In spite of the lower polymerization temperature in the mixture of $\epsilon\text{-ACA}$ with **1**, a processing temperature of 230°C was chosen for hybrid material synthesis because of the high melting point of PA6 (220°C).

The overall process for synthesizing PA6/SiO₂ hybrid materials has been carried out in a high pressure autoclave suitable for PA6 synthesis (Experimental Part). It must be mentioned, that the order of reactant addition can be varied. Pre-polymerization of the reactants $\epsilon\text{-ACA}$ and $\epsilon\text{-CL}$ and subsequent addition of **1** is possible, but products show discoloration due to contact with air while heating. Reaction time and polymerization temperature are important for homogeneity and extractable amounts, so that for a better comparability all experiments are done with constant reaction conditions in an autoclave. All reactants are inserted at the beginning of the heating period and the reactions are done under inert atmosphere at a temperature of 230°C for 3.5 h including the heating and post condensation phase. For further information see Table S7 in ESI†.

The observed extractables of the hybrid materials amount 10–32 % and depend on the molar ratios of reactants (Table 1). Especially for the samples **P1** and **P5** a decreasing amount of extractables can be detected with a higher $\epsilon\text{-ACA}$ ratio. The resulting PA6/SiO₂ hybrid materials are homogeneous solid materials (Fig. 3). Primary monolithic products were received but also granules can be fabricated. Furthermore, the resulting thermoplastic materials can be extruded to films.

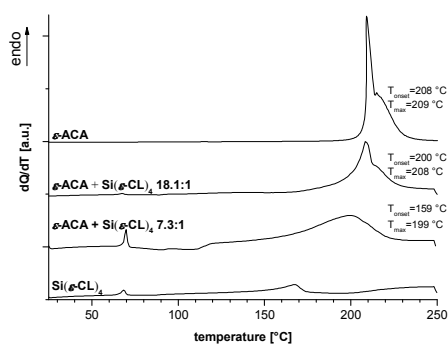


Fig. 2 DSC curves of mixtures of $\epsilon\text{-ACA}$ with **1** in different molar ratios at a heating rate of $10\text{ K}\cdot\text{min}^{-1}$.



Fig. 3 Images of PA6/SiO₂ hybrid materials according to sample **P2** (Experimental Part, Table 1) as monolith, granules and film.

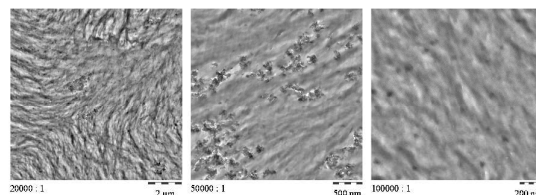


Fig. 4 TEM images of a monolithic sample of **P2** after freezing ultra thin cuts in different magnifications.

Table 2 Electron microscopic images and EDX patterns of hybrid materials with 1, 2 and 5 wt% of SiO₂ in different magnifications; EDX showing the distribution of the elements nitrogen, oxygen, carbon and silicon.

Sample (SiO ₂ amount)	Electron microscopy Picture
P1_1 (1 wt%) Molar ratio ε-ACA Si(ε-CL) ₄ 10 1	
P1_2 (1 wt%) Molar ratio ε-ACA Si(ε-CL) ₄ 7.2 1	
P1_3 (1 wt%) Molar ratio ε-ACA Si(ε-CL) ₄ 4 1	
P2* (2 wt%) Molar ratio ε-ACA Si(ε-CL) ₄ 4.3 1	
P5_1 (5 wt%) Molar ratio ε-ACA Si(ε-CL) ₄ 4 1	
P5_2 5 wt%	

* The obtained element fluorine is due to the mechanical crushing of composite material after polymerization process in the used Teflon beaker.

TEM images of **P2** show SiO₂ agglomerates with primary particles of 35–60 nm in size (Fig. 4).

Homogeneity of samples as well as agglomeration tendency are affected by the containing SiO₂ amount as can be seen from electron microscopic images (Table 2 and Fig. S4–Fig. S9 in ESI†). The higher the SiO₂ content which is formed during polymerization, the more agglomeration of inorganic particles can be observed. The resulting SiO₂ agglomerates build particles with different shapes for example up to 30 μm long needle-like (**P1_1**) or shell-like particles around hybrid material (**P5_1**) but often spherical as can be seen from the other examples. At highest SiO₂ content (**P5_2**) particles larger than 100 μm are obtained. Furthermore, molar ratios of reactants seem to have an influence on agglomeration tendency. Hence, for example at experiment with constant SiO₂ amount (**P1** and **P5**) an increasing ε-ACA ratio causes a decrease of SiO₂ particle size. The obtained wide particle size distribution could have influence on mechanical behavior but this is part of further work.

The solid state ¹³C and ²⁹Si NMR spectra of the hybrid materials **P2** evidence the molecular structure which relates to the PA6/SiO₂ (Fig. 5). The solid state ¹³C NMR spectrum is in agreement with literature data of pure PA6 high in α-crystallinity.⁴⁶ The solid state ²⁹Si NMR spectrum of the hybrid material shows Q₃ and Q₄ signals, which indicate Si atoms bound to 3 or 4 other Si atoms over siloxane-bridges. It is not possible to distinguish if the Q₃ signal is caused by Si–OH or Si–OC groups. Therefore, bonding of carboxylic acid groups to silicon cannot be excluded.

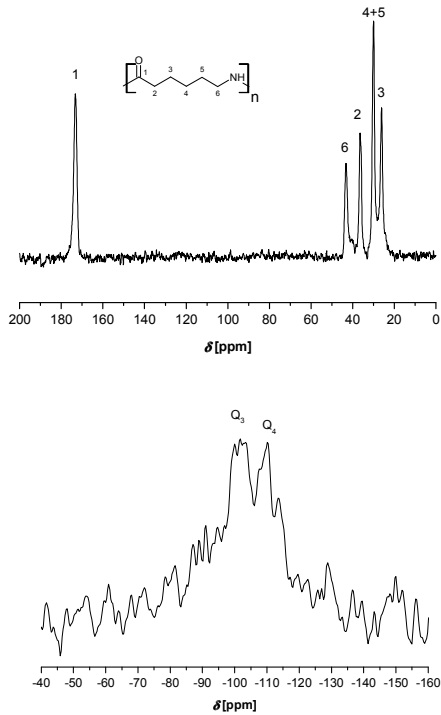


Fig. 5 Solid state ¹³C{¹H}-CP-MAS (above) and ²⁹Si{¹H}-CP-MAS NMR spectra (below) of a 2 wt% SiO₂ sample **P2**.

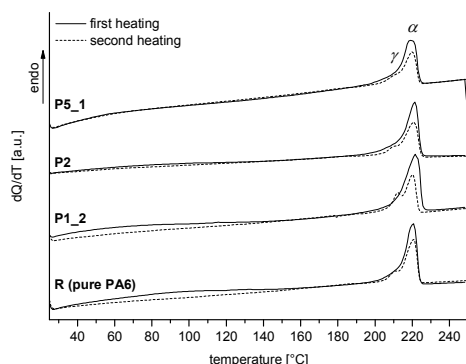


Fig. 6 First and second heating of a cyclic DSC measurement of pure polyamide 6 in comparison to hybrid materials with 1, 2 and 5 wt% of SiO₂ (extracted samples); signals of α - and γ -crystal modification are marked.

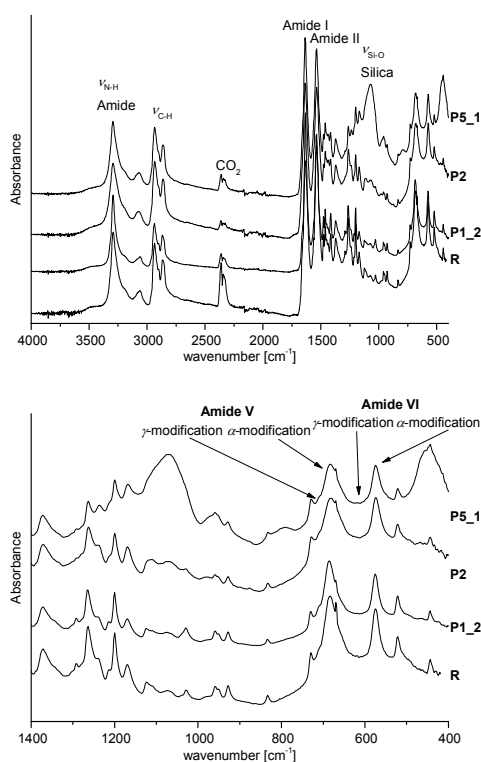


Fig. 7 ATR-FTIR spectra of hybrid materials with 1, 2 and 5 wt% of SiO₂ in comparison to pure polyamide 6 (extracted samples); above: full wavenumber range; below: fingerprint region.

DSC traces of the samples **R**, **P1_1**, **P2** and **P5_1** show the typical thermal behavior of thermoplastic PA6 with a melting point around 220 °C (Fig. 6).

As already described for the solid state ¹³C NMR spectra, the crystallinity of PA6 is predominated by α -modification. Variation of the SiO₂ amount has no influence on the melting or crystallization temperature and the crystal modification. The degree of crystallization with values between 30–40 % is independent of the SiO₂ content and indicates the presence of crystalline and amorphous regions in the organic polymer. For

further information see Table S8 (ESI[†]). Independent of the SiO₂ amount, all samples show similar thermal decomposition behavior (thermogravimetric analysis, Fig. S4, ESI[†]).

In agreement to solid state ¹³C NMR and ²⁹Si spectra and DSC measurements, ATR-FTIR spectra indicate typical bands for polyamide 6 like Amide I band at 1636 cm⁻¹ and Amide II band at 1536 cm⁻¹ as well as N–H at 3295 cm⁻¹. Furthermore the typical Si–O stretching vibration at 1073 cm⁻¹ for SiO₂ is observed (see Fig. 7). Additionally the ATR-FTIR spectra give information about the crystallization behavior of PA6. The position of the Amide V band at 690 cm⁻¹ and Amide VI band at 580 cm⁻¹ indicate crystallization mainly in α -modification as evidenced from DSC and solid state ¹³C NMR measurements, too. Amorphous polymer shows broad signals, which can also be observed. Crystallization in the γ -modification would induce bands at 712 cm⁻¹ and 625 cm⁻¹ for Amid V and VI.^{47–49}

For additional characterization of the obtained hybrid materials the molar mass of the obtained PA6 and the influence of post condensation on the molecular weights and the polydispersity index (PDI) were investigated by size exclusion chromatography (SEC, Table 3, Fig. 8 and Fig. S14 in ESI). All polymers show a monomodal distribution of the molar mass. The SiO₂ content seems to have a slight influence on molecular weight and its distribution. Therefore M_w as well as M_n and PDI increase with increasing the SiO₂ amount that

Table 3 SEC results of hybrid materials with 1 wt%, 2 wt% before and after post condensation and 5 wt% of SiO₂ content in comparison to PA6; extracted samples.

Sample	M_w	M_n	PDI
Reference (pure PA6)	48,000	17,500	2.7
P1_1	54,000	18,900	2.9
P1_2	46,200	17,500	2.6
P1_3	35,800	14,400	2.5
P2; 2 wt% SiO₂	49,700	17,400	2.8
Before post condensation			
P2post; 2 wt% SiO₂	104,000	19,200	5.4
After post condensation			
P5_1	62,600	19,900	3.1
P5_2	80,100	22,900	3.5

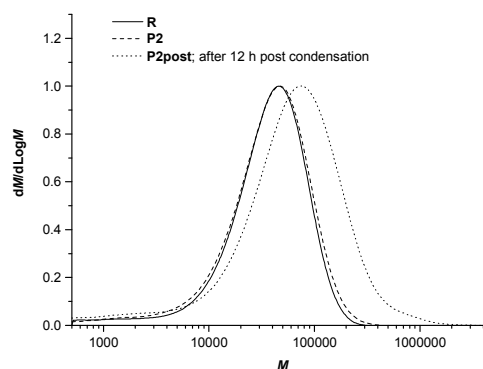


Fig. 8 SEC profiles of hybrid material **P2** with 2 wt% of SiO₂ before and after post condensation at 200 °C and 5 mbar for 12 h in comparison to the PA6 as reference; extracted samples (48 h, MeOH); normalized to peak height.

attends with an arising ratio of ε -ACA in comparison to the other reactants, namely **1** and ε -caprolactam. Generally, high amino acid concentrations lead to an increasing reaction rate of polycondensation reaction and therefore higher chain lengths and higher conversion. For example, a decrease in ε -ACA:1 ratio for **P1_1** to **P1_3** causes a decrease in obtained molar mass due to a reduced conversion of the reactants. A diametrical effect is determined for **P5_1** and **P5_2**. It must be mentioned, that for these cases a higher ε -ACA content leads to lower chain lengths due to a decrease of ε -caprolactam unit amount and a higher concentration of amino or carboxylic acid end groups.

As expected, the post condensation reaction of **P2** at 200 °C leads to much higher M_w . Additionally, a broader distribution of the molar masses with a higher PDI after post condensation is observed. This is due to the not reached equilibrium of the post condensation reaction. Additionally, the water content in the polymer grains decreases from the inner to the outer sphere. Therefore a different molecular weight distribution over the polymer grain is ascertained.⁵⁰ In some cases a microscopic nonuniformity of the solid polymers, especially a distribution of crystallite sizes, is discussed as a further reason.⁵¹

Kinetic and thermodynamic investigations of the presented polymerization type are still under study.

Conclusions

In this study polyamide 6/SiO₂ hybrid materials were produced by a coupled polymerization reaction of three monomeric components namely 1,1',1'',1'''-silanetetrayltetrakis-(azepan-2-one), 6-aminocaproic acid and ε -caprolactam within one process. The amount of SiO₂ is tunable by variation of reactant stoichiometry, whereas the ratio of 1,1',1'',1'''-silanetetrayltetrakis-(azepan-2-one) to 6-aminocaproic acid is of great importance for a high conversion and homogeneity.

The investigations have shown that the filler has no significant effect on thermal properties. The average molecular weight slightly rises with increasing the SiO₂ content. Furthermore, the latter increased during post condensation reaction and, additionally, a broader PDI was determined. Examination of the crystallization behavior of the obtained PA6 by NMR as well as FTIR spectroscopy and DSC show a predominated α -crystallinity and amorphous regions. Unfavorable is the increasing agglomeration tendency of the primary nanoparticles with higher SiO₂ amounts. In contrast to conventional *in situ* procedures or the compounding for the synthesis of PA6/filler hybrid materials, the preceding modification of the filler and negative effects of modifier, like the thermal degradation,^{52,53} can be omitted with the described method. Additionally, problems in terms of processing potential toxic nanoparticle powders are avoided.⁵⁴

Acknowledgments

We thank Fonds der Chemischen Industrie and Deutsche Forschungsgemeinschaft (DFG Sp 392/39–1) for financial support. Furthermore we acknowledge R. John, M. Martin and T. Windberg for their experimental work. We thank Prof. Hietschold and T. Jagemann (TU Chemnitz) for measuring respectively the opportunity of measuring Electron microscopic images.

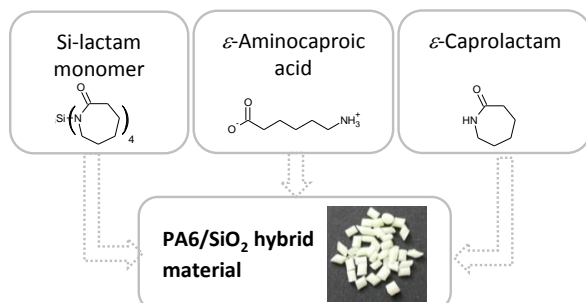
References

- 1 S. Geier and C. Bonten, *Polym. Eng. Sci.*, 2014, **54**, 247–254.
- 2 Y. Kojima, A. Usuki, M. Kawasumi, A. Okada, Y. Fukushima, T. Kurauchi and O. Kamigaito, *J. Mater. Res.*, 1993, **8**, 1185–1189.
- 3 Y. Kojima, A. Usuki, M. Kawasumi, A. Okada, T. Kurauchi and O. Kamigaito, *J. Polym. Sci., Part A: Polym. Chem.*, 1993, **31**, 983–986.
- 4 K. Masenelli-Varlot, E. Reynaud, G. Vigier and J. Varlet, *J. Polym. Sci., Part B: Polym. Phys.*, 2002, **40**, 272–283.
- 5 T. J. Bessell and J. B. Shortall, *J. Mater. Sci.*, 1977, **12**, 365–372.
- 6 S.-H. Wu, F.-Y. Wang, C.-C. M. Ma, W.-C. Chang, C.-T. Kuo, H.-C. Kuan and W.-J. Chen, *Mater. Lett.*, 2001, **49**, 327–333.
- 7 K. Han, Z. Liu and M. Yu, *Macromol. Mater. Eng.*, 2005, **290**, 688–694.
- 8 A. Güllü, A. Özdemir and E. Özdemir, *Mater. Des.*, 2006, **27**, 316–323.
- 9 B. Ou, Z. Zhou, Q. Liu, B. Liao, Y. Xiao, J. Liu, X. Zhang, D. Li, Q. Xiao and S. Shen, *Polym. Compos.*, 2014, **35**, 294–300.
- 10 H. R. Pant, M. P. Bajgai, K. T. Nam, Y. A. Seo, D. R. Pandeya, S. T. Hong and H. Y. Kim, *J. Hazard. Mater.*, 2011, **185**, 124–130.
- 11 M. Zhu, Q. Xing, H. He, Y. Zhang, Y. Chen, P. Pötschke and H.-J. Adler, *Macromol. Symp.*, 2004, **210**, 251–261.
- 12 A. D. Erem, G. Ozcan and M. Skrifvars, *Text. Res. J.*, 2011, **81**, 1638–1646.
- 13 I. B. Page, *Polyamides as Engineering Thermoplastic Materials*, iSmithers Rapra Publishing, 2000, vol. 11, p. 13.
- 14 L. Shen, Q. Du, H. Wang, W. Zhong and Y. Yang, *Polym. Int.*, 2004, **53**, 1153–1160.
- 15 Y. Ou, F. Yang and Z.-Z. Yu, *J. Polym. Sci., Part B: Polym. Phys.*, 1998, **36**, 789–795.
- 16 M. Nanko, *Advances in Technology of Materials and Materials Processing*, 2009, **11**, 1–8.
- 17 M. García, J. Barsema, R. E. Galindo, D. Cangialosi, J. Garcia-Turiel, W. E. van Zyl, H. Verweij and D. H. A. Blank, *Polym. Eng. Sci.*, 2004, **44**, 1240–1246.
- 18 M. M. Hasan, Y. Zhou, H. Mahfuz and S. Jeelani, *Mater. Sci. Eng., A*, 2006, **429**, 181–188.
- 19 V. N. Dougnac, B. C. Peoples and R. Quijada, *Polym. Int.*, 2011, **60**, 1600–1606.
- 20 P. Theil-Van Nieuwenhuysse, V. Bounor-Legaré, P. Bardollet, P. Cassagnau, A. Michel, L. David, F. Babonneau and G. Camino, *Polym. Degrad. Stab.*, 2013, **98**, 2635–2644.
- 21 W. E. van Zyl, M. García, B. A. G. Schrauwen, B. J. Kooi, J. T. M. De Hosson and H. Verweij, *Macromol. Mater. Eng.*, 2002, **287**, 106–110.
- 22 M. García, G. van Vliet, M. G. J. ten Cate, F. Chávez, B. Norder, B. Kooi, W. E. van Zyl, H. Verweij and D. H. A. Blank, *Polym. Adv. Technol.*, 2004, **15**, 164–172.
- 23 F. Yang, Y. Ou and Z. Yu, *J. Appl. Polym. Sci.*, 1998, **69**, 355–361.

- 24 Y. Li, J. Yu and Z.-X. Guo, *J. Appl. Polym. Sci.*, 2002, **84**, 827–834.
- 25 L. F. Cai, *EXPRESS Polym. Lett.*, 2010, **4**, 397–403.
- 26 G. Rusu and E. Rusu, *High Perform. Polym.*, 2006, **18**, 355–375.
- 27 H. Gu, Y. Guo, S. Y. Wong, Z. Zhang, X. Ni, Z. Zhang, W. Hou, C. He, V. P. W. Shim and X. Li, *Microporous Mesoporous Mater.*, 2013, **170**, 226–234.
- 28 J. Liu, H. Yi, H. Lin, T. Wei and B. Zheng, *Polym. Compos.*, 2014, **35**, 435–440.
- 29 C. Zhao, P. Zhang and S. Lu, *J. Mater. Sci.*, 2007, **42**, 9083–9091.
- 30 S. Spange and S. Grund, *Adv. Mater.*, 2009, **21**, 2111–2116.
- 31 M. W. Ellsworth and B. M. Novak, *J. Am. Chem. Soc.*, 1991, **113**, 2756–2758.
- 32 B. M. Novak and C. Davies, *Macromolecules*, 1991, **24**, 5481–5483.
- 33 M. W. Ellsworth and B. M. Novak, *Chem. Mater.*, 1993, **5**, 839–844.
- 34 B. M. Novak, *Adv. Mater.*, 1993, **5**, 422–433.
- 35 S. Grund, P. Kempe, G. Baumann, A. Seifert and S. Spange, *Angew. Chem.*, 2007, **119**, 636–640.
- 36 S. Spange, P. Kempe, A. Seifert, A. A. Auer, P. Ecorchard, H. Lang, M. Falke, M. Hietschold, A. Pohlers, W. Hoyer, G. Cox, E. Kockrick and S. Kaskel, *Angew. Chem.*, 2009, **121**, 8403–8408.
- 37 T. Ebert, A. Seifert and S. Spange, *Macromol. Rapid Commun.*, **2015**, DOI 10.1002/marc.201500182.
- 38 K. Hedberg, *J. Am. Chem. Soc.*, 1955, **77**, 6491–6492.
- 39 J. He, J. F. Harrod and R. Hynes, *Organometallics*, 1994, **13**, 2496–2499.
- 40 N. W. Mitzel, A. Schier, H. Beruda and H. Schmidbaur, *Chem. Ber.*, 1992, **125**, 1053–1059.
- 41 N. Mitzel, A. Schier and H. Schmidbaur, *Chem. Ber.*, 1992, **125**, 2711–2712.
- 42 A. Bondi, *J. Phys. Chem.*, 1964, **68**, 441–451.
- 43 Markus Wollenweber, Keese, Reinhart and Stoeckli-Evans, Helen, *Z. Naturforsch.*, 1998, **53 b**, 145–148.
- 44 G. Rong, R. Keese and H. Stoeckli-Evans, *Eur. J. Inorg. Chem.*, 1998, **1998**, 1967–1973.
- 45 F. Carre, C. Chuit, R. J. P. Corriu, A. Fanta, A. Mehdi and C. Reye, *Organometallics*, 1995, **14**, 194–198.
- 46 G. R. Hatfield, J. H. Glans and W. B. Hammond, *Macromolecules*, 1990, **23**, 1654–1658.
- 47 A. Miyake, *J. Polym. Sci.*, 1960, **44**, 223–232.
- 48 M. I. Kohan, Ed., *Nylon plastics handbook*, Hanser Publishers, Munich; New York: Cincinnati, 1995.
- 49 I. Matsubara and J. H. Magill, *Polymer*, 1966, **7**, 199–215.
- 50 K. Meyer, *Angew. Makromol. Chem.*, 1973, **34**, 165–167.
- 51 J. Zimmermann, *J. Polym. Sci., Part C: Polym. Lett.*, 1964, **2**, 955–958.
- 52 W. Xie, Z. Gao, W.-P. Pan, D. Hunter, A. Singh, Anant and R. Vaia, *Chem. Mater.*, 2001, **13**, 2979–2990.
- 53 T. D. Fornes, P. J. Yoon and D. R. Paul, *Polymer*, 2003, **44**, 7545–7556.
- 54 D. Napierska, L. C. Thomassen, D. Lison, J. A. Martens and P. H. Hoet, *Particle and Fibre Toxicology*, 2010, **7**, 39.

Polyamide 6/silica hybrid materials by a coupled polymerization reaction

L. Kaßner, K. Nagel, R.-E. Grützner, M. Korb, T. Rüffer, H. Lang and S. Spange



Polyamide 6/SiO₂ hybrid materials with an adjustable SiO₂ amount were produced by the coupled polymerisation of three monomeric components namely 1,1',1'',1'''-silanetetrayltetrakis-(azepan-2-one), 6-aminocaproic acid and ε-caprolactam within one process.